

See discussions, stats, and author profiles for this publication at: <https://www.researchgate.net/publication/26288402>

Converse Flexoelectric Effect in Bent-Core Nematic Liquid Crystals

ARTICLE in THE JOURNAL OF PHYSICAL CHEMISTRY B · JULY 2009

Impact Factor: 3.3 · DOI: 10.1021/jp903241z · Source: PubMed

CITATIONS

31

READS

59

7 AUTHORS, INCLUDING:



Pramoda Kumar

Harvard University

15 PUBLICATIONS 122 CITATIONS

SEE PROFILE



Uma Hiremath

Centre for Nano and Soft Matter Sciences

52 PUBLICATIONS 597 CITATIONS

SEE PROFILE



K. S. - Krishnamurthy

Centre for Nano and Soft Matter Sciences (...)

41 PUBLICATIONS 239 CITATIONS

SEE PROFILE



Alexander Georgiev Petrov

Bulgarian Academy of Sciences

124 PUBLICATIONS 1,450 CITATIONS

SEE PROFILE

Converse Flexoelectric Effect in Bent-Core Nematic Liquid Crystals

Pramoda Kumar,[†] Y. G. Marinov,[‡] H. P. Hinov,[‡] Uma S. Hiremath,[†] C. V. Yelamaggad,[†] K. S. Krishnamurthy,^{*,†} and A. G. Petrov^{*,‡}

Centre for Liquid Crystal Research, P.O. Box 1329, Jalahalli, Bangalore 560 013, India, and Institute of Solid State Physics, Bulgarian Academy of Sciences, 72 Tzarigradsko Chaussee, Sofia 1784, Bulgaria

Received: April 8, 2009; Revised Manuscript Received: May 13, 2009

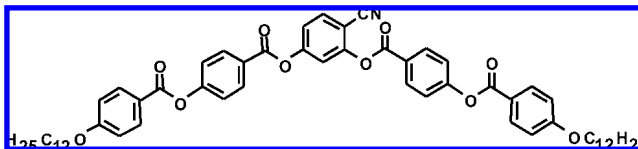
We report on the converse flexoelectric effect in two bent-core nematic liquid crystals with opposite dielectric anisotropies. The results are based on electro-optic investigations of inplane field-driven distortions in homeotropic samples (the Helfrich method). They are interpreted by an extension of the Helfrich theory that takes into account the higher order distortions. The bend flexocoefficient for both the compounds is of the usual order of magnitude as in calamitics, unlike in a previously investigated bent-core nematic for which giant values of the bend flexocoefficient are reported. In order to resolve this discrepancy, we propose a molecular model with nonpolar clusters showing quadrupolar flexoelectricity. The study also includes measurements on surface polarization instabilities in the dielectrically positive material; the splay flexocoefficient thereby deduced is also of the conventional order.

Introduction

Flexoelectricity is an important mechano-electric property of liquid crystals (LCs) that provides a reciprocal relationship between curvature distortions and electric polarization.¹ The polarization **P** generated in a nematic liquid crystal by curvature deformations of the director **n** follows the relation $\mathbf{P} = e_{1z}(\nabla \cdot \mathbf{n})\mathbf{n} + e_{3x}(\nabla \times \mathbf{n}) \times \mathbf{n}$, with e_{1z} and e_{3x} denoting the splay and bend flexoelectric coefficients, respectively. While commonly measured flexocoefficients are in the range of a few pC m⁻¹ for calamitic nematic LCs,¹ recently, a giant e_{3x} of the order of tens of nC m⁻¹ has been measured in the bent-core nematic 4-chloro-1,3-phenylene bis[4'-(9-decenyloxy)benzoyloxy]benzoate (CIPbis10BB) by studying the direct flexoeffect of the material sandwiched between flexible electrodes.² Further, this giant value has been reconfirmed by the converse flexoeffect: appearance of a substantial electric field-induced bending in a bent-core (BC) nematic sample confined between the same type of flexible electrodes.³ On the other hand, a recent determination of e_{3x} by the Helfrich method,⁴ which involves electrically induced bending of a homeotropic nematic layer, provides for the very same compound a value having just the usual order of magnitude.⁵ In view of these conflicting results, we considered it important to examine the flexoelectric behavior of other BC nematics so as to arrive at a broader understanding of the experimental situation. Accordingly, we have measured e_{3x} by the Helfrich method,^{4,6} for two BC mesogens with opposite signs of dielectric anisotropy; we have also determined the total flexocoefficient ($e_{1z} + e_{3x}$) of these materials by extending the Helfrich theory to larger electric fields and by experiments on polar surface instability⁷ in the dielectrically positive material. We find that, for both the compounds, e_{3x} is of conventional order. In order to resolve this discrepancy, we propose a cluster molecular model with the clusters exhibiting quadrupolar flexoelectricity.

Experimental Methods

A. Measurements on CNRbis12OBB. One of the BC compounds studied here, 4-cyanoresorcinol bis[4-(4-n-dodecyloxybenzoyloxy)benzoate] (CNRbis12OBB), is a mesogen first synthesized by Kovalenko et al.⁸ and having the chemical structure:



Its reported⁸ phase sequence is Cr 103 °C (SmCP_A' 68 °C SmCP_A' 75 °C SmCP_A 94 °C) SmC 109 °C N 129 °C I, with Cr, SmCP_A, SmC, N, and I denoting, respectively, the crystal, antipolar smectic C, smectic C, nematic, and isotropic phases. The compound synthesized by us showed a lower clearing temperature of 125 °C, while its nematic range remained the same as in ref 8.

For the measurement of e_{3x} , the sample cells were constructed by sandwiching two parallel aluminum strip electrodes, spaced about 2 mm apart, between octadecyltriethoxysilane treated nonconducting glass plates. Two Mylar strips, with the electrodes located between them, were heat sealed to the glass plates by cooling from ca. 250 °C under a uniform pressure; this ensured rigidity of the assembly, with the sample thickness *d* nearly the same as the thickness of the aluminum strips. The *d* value was precisely determined interferometrically using a grating spectrometer. The sample in its isotropic phase was drawn into the cell by capillary action and then cooled slowly through the isotropic–nematic transition temperature. The homeotropic orientation of the director was confirmed by conoscopic observations. For optical observations, a Carl-Zeiss Axio Imager M1m polarizing microscope equipped with an AxioCam MRC 5 digital camera was used. The sample temperature was maintained at 120 °C by a Mettler FP90 hot-stage. The voltage source was a Stanford Research Systems DS 345 function generator

* Corresponding authors. E-mail: murthyksk@gmail.com (K.S.K.); director@issp.bas.bg (A.G.P.).

[†] Centre for Liquid Crystal Research.

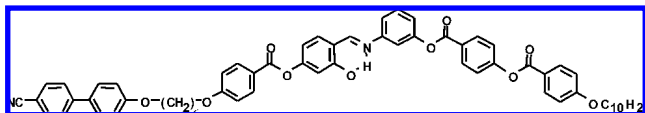
[‡] Bulgarian Academy of Sciences.

coupled to a FLC Electronics voltage amplifier (Model F20ADI). The applied voltage V was measured with a HP 34401A multimeter.

CNRbis12OBB is a negative dielectric anisotropy material. Its bend elastic constant K_{33} was determined from electric Freedericksz transition data on homeotropic samples. For these measurements, we have used sandwich cells of silane treated ITO-coated glass plates. An Agilent 4284A precision LCR meter was employed to monitor the cell capacitance. While the permittivity parallel to the nematic director ϵ_{\parallel} was calculated from the initial capacitance C_{\parallel} , that perpendicular to the director ϵ_{\perp} was determined from the capacitance C_{\perp} corresponding to infinite field, obtained by a suitable extrapolation of the $C(V^{-1})$ line.

For birefringence (Δn) measurements, a $5\ \mu\text{m}$ thick planar sample sandwiched between polyimide coated and unidirectionally buffed glass plates was used; the optical retardation was measured with a Berek compensator.

B. Measurements on BCCB. The second liquid crystal compound studied here, 4-((3-(4-(4-(decyloxy)benzoyloxy)benzoyloxy)phenylimino)methyl)-3-hydroxyphenyl 4-(6-(4'-cyano-biphenyl-4-yloxy)hexyloxy)benzoate (**BCCB**), consists of a salicyladimine-based BC mesogen covalently linked through a hexamethylene spacer to a rod-like cyanobiphenyl (CB) unit. Its chemical structure is



The phase sequence of **BCCB** on cooling is reported⁹ to be I 162 °C N_b 135.6 °C SmA_b 119.2 °C M 105.5 °C Cr, with I, N_b, SmA_b, and Cr denoting isotropic, biaxial nematic, biaxial smectic and crystal phases, in that order; M stands for an unidentified layered structure. Measurements were performed at 140 °C in the nematic phase. In our flexoelectric experiments concerning the N phase, we did not come across any feature that could be ascribed to the conjectured biaxiality and the homeotropic samples in the field-off state always displayed a uniaxial cross in converging light. Thus, we treat the N phase examined as of uniaxial symmetry.

In **BCCB**, a sickle-shaped compound, the longitudinal CN dipole renders the material dielectrically positive. More importantly to the phenomenon under study, it gives rise to a surface polarization m_p that, together with curvature-induced polarization, leads to an apparent flexocoefficient ($e_{3x} + m_p$).¹ We determined ($e_{3x} + m_p$) by the Helfrich method, employing an interference polarizing microscope MPI-5 (PZO) in the differential regime of measurement of optical path difference. The results confirm the classical order of magnitude ($\sim \text{pC m}^{-1}$) for e_{3x} as in ordinary calamitics (see below).

Furthermore, we determined the total flexocoefficient along with surface polarization ($e_{1z} + e_{3x} + m_p$) for **BCCB** using the method of dielectric quenching of the surface polar instability.⁷ For this purpose, homeotropic cells with transparent conductive ITO electrodes were prepared, and the polar instability was observed under a Carl-Zeiss Axio Imager. The electrode position of the instability was unambiguously located by moving the focal plane using the motorized stage movement with the minimum step size of $0.01\ \mu\text{m}$.

Theory

A. Flexoelectric Bending in a Homeotropic Layer. This effect takes place when a homeotropic layer is subjected to an

electric field E orthogonal to the director. Its first observation in the homeotropic 4-methoxybenzylidene-4'-*n*-butylaniline (MBBA) layer¹¹ remained unexplained until a theory based on flexoelectricity was developed for its analysis.⁴ Subsequently, detailed experiments were performed with nematic MBBA⁶ confirming most of the theoretical predictions. However, the experimental results in ref 11 produced a value of e_{3z} for MBBA that differed from the value in ref 6; this discrepancy was later accounted for^{12,13} by considering the effect of surface polarization m_p . With asymmetric end substituents of the LC molecule (hydrophilic/hydrophobic asymmetry), m_p may have an opposite sign for homeotropically orienting glass plates that are hydrophilic¹¹ or hydrophobic.⁶ A complete theory of 1D dielectric–flexoelectric deformations of nematic layers was subsequently developed.¹² The conclusion of this theory was that the flexoelectric bending is not determined exclusively by the bend flexocoefficient e_{3x} but by the apparent flexocoefficient $e_{3x}^* = e_{3x} + m_p$.

The solution routinely used for interpreting experimental data on flexoelectric bending in a homeotropic layer reads⁶

$$\Delta l = n_o \left(1 - \frac{n_o^2}{n_e^2} \right) \left(\frac{d\theta}{dz} \right)^2 \frac{d^3}{24} \quad \text{with } d\theta/dz = e_{3x}^* E / K_{33} \quad (1)$$

where Δl is the optical path difference, d the sample thickness, θ the director deviation from its initial direction z , E the applied field, and K_{33} the bend elastic constant; n_o and n_e are the ordinary and extraordinary refractive indices. When the birefringence $\Delta n = (n_e - n_o)$ is very small, eq 1 simplifies to $\Delta l = \Delta n (d\theta/dz)^2 (d^3/12)$. However, this equation holds under the assumption of small deformations (linear approximation), vanishing anchoring strength W and zero dielectric anisotropy $\Delta\epsilon = \epsilon_{\parallel} - \epsilon_{\perp}$. In the event of the last two assumptions not holding good, the following approximate solution⁴ could account for them:

$$\Delta l = \Delta n \left(\frac{d\theta}{dz} \right)^2 \frac{d^3}{12} = \Delta n \left(\frac{e_{3x}^*}{K_{33}} \right)^2 E_{\text{eff}}^2 \frac{d^3}{12} \quad (2)$$

where

$$E_{\text{eff}}^2 = \frac{E^2}{\left(1 + \frac{d}{2b} - \frac{\Delta\epsilon \epsilon_o E^2 d^2}{12 K_{33}} \right)^2} \quad (3)$$

with $b = K_{33}/W$ as the extrapolation length and ϵ_o as the free-space permittivity.

We generalize the above Helfrich model by considering the anisotropy in elastic and flexoelectric parameters in the following manner. The “electric enthalpy” functional H_v is minimized by the approximate Ritz method. $\theta(z)$ is taken as linear in z , and the integrand of the electric enthalpy is expanded up to the second order in θ .

$$H_v = \frac{1}{2}(K_{11} \sin^2 \theta + K_{33} \cos^2 \theta) \left(\frac{d\theta}{dz} \right)^2 + (e_{1z} \sin^2 \theta - e_{3x} \cos^2 \theta) E \frac{d\theta}{dz} - \frac{1}{2} \epsilon_0 (\epsilon_{11} \sin^2 \theta + \epsilon_{\perp} \cos^2 \theta) E^2 \approx \frac{1}{2} (K_{33} + \Delta K \theta^2) \left(\frac{d\theta}{dz} \right)^2 - (e_{3x} - e_+ \theta^2) E \frac{d\theta}{dz} - \frac{1}{2} \epsilon_0 (\epsilon_{\perp} + \Delta \epsilon \theta^2) E^2 \quad (4)$$

The appearance of the splay flexocoefficient comes from relaxing the limitation of small deformations (i.e., $\theta^2 \sim 0$) made earlier.^{3,6} When the director deviation at the surface becomes large, as for instance when $\theta(d/2) = \pi/4$, the deformation at the surface is predominantly splay, while in the midplane it is mostly bent. Thus, the effect of both flexocoefficients is important at higher electric fields.

After performing the integration over z , the “electric enthalpy” functional is expressed in terms of the constant $d\theta/dz$ by using $\int_{-d/2}^{d/2} \theta^2(z) dz = (d\theta/dz)^2 d^3/12$. To the bulk contribution, surface terms are properly added, i.e., $+W \theta(d/2) - 2m_p E \theta(d/2)$, and the relationship $\theta(d/2) = (d\theta/dz)d/2$ is applied. Now, we may account for the anisotropy of bend and splay flexoelectric coefficients ($e_+ = e_{1z} + e_{3x} \neq 0$) by retaining the terms up to $(d\theta/dz)^3$ in the resulting function, and of the anisotropy of the elastic constants ($\Delta K = K_{11} - K_{33} \neq 0$), by the terms up to $(d\theta/dz)^4$. By minimizing such a function form of the electric enthalpy, we obtain a quadratic equation in $(d\theta/dz)$ in the first case and a cubic one in the second case. The solutions of these equations, in effect, bring in small correction terms Δ_1 and Δ_2 into eq 2. Thus, for $e_+ \neq 0$ and $\Delta K \neq 0$ in the limit of small E , we have

$$\Delta l = \Delta n \left(\frac{e_{3x}^*}{K_{33}} \right)^2 E_{\text{eff}}^2 \frac{d^3}{12} [1 - (\Delta_1 + \Delta_2) E_{\text{eff}}^2]^2 \quad (5)$$

where $\Delta_1 = \frac{1}{4} \left(\frac{e_+ e_{3x}^*}{K_{33}^2} \right) d^2$ and $\Delta_2 = \frac{1}{3} \frac{\Delta K}{K_{33}} \left(\frac{e_{3x}^*}{K_{33}} \right)^2 \frac{d^2}{1 + d/2b}$ (6)

B. Dielectrically Suppressed Flexoelectric Bending and Surface Polar Effects in a Homeotropic Layer. The dielectric torque has been shown¹³ to suppress the flexoelectric bending in negative $\Delta \epsilon$ nematics studied in the transverse geometry ($\mathbf{E} \perp \mathbf{n}$). Thus, we may estimate W , e_{3x}^* , and e_+ in negative $\Delta \epsilon$ nematics by measuring the optical path change Δl under simultaneous action of ac and dc fields. Now, eq 3 modifies to

$$E_{\text{eff}}^2 = \frac{E_{\text{dc}}^2}{\left(1 + \frac{d}{2b} - \frac{\Delta \epsilon \epsilon_0 (E_{\text{dc}}^2 + E_{\text{ac}}^2) d^2}{12 K_{33}} \right)^2} \quad (7)$$

The dielectric torque also suppresses the surface polar instability in positive $\Delta \epsilon$ nematics studied in the longitudinal geometry ($\mathbf{E} \parallel \mathbf{n}$).^{7,13} Thus, by applying a sufficiently strong ac field simultaneously with the dc field, the instability being driven only by the latter may be completely quenched. The quenching data enable determination of both the surface extrapolation length b and the apparent total flexocoefficient $e_+^* = (e_{1z} + e_{3x} + m_p)$ given by the following simplified expressions⁷ based on the general theory by Petrov et al.¹³

$$b = d \sqrt{\frac{K_{33}}{\epsilon_0 \Delta \epsilon}} \frac{1}{V_{\text{ac}}} \frac{\Delta V_{\text{dc}}}{V_{\text{dc}}^0} \quad (8)$$

and

$$e_+^* = \sqrt{\epsilon_0 \Delta \epsilon K} \left(1 + \frac{V_{\text{ac}}}{\Delta V_{\text{dc}}} \right) \quad (9)$$

Here, V_{dc}^0 is the dc instability threshold in the absence of ac, V_{ac} is the rms value of the ac voltage applied simultaneously with the dc voltage, and ΔV_{dc} is the enhancement of the dc threshold under the action of the corresponding ac voltage V_{ac} .

Results and Discussion

For convenience, in describing the electro-optical bending, we take the observation direction as z and the normal to electrodes (field direction) as x ; the setting of the polarizer P crossed with respect to the analyzer A will be indicated as P(ψ)–A($90+\psi$), ψ being the angle made by the transmission axis of the polarizer with x .

A. The Flexocoefficients in CNRbis12OBB. Under orthoscopic illumination, in the initial field-off state, the sample appears extinct between crossed polarizers P(ψ)–A($90+\psi$) for all angles ψ , and in convergent beam, it displays a uniaxial cross. On applying a small in-plane dc field, in parallel beam and between diagonally crossed polarizers P(45)–A(135), uniform birefringence with maximum transmission is observed, and the higher of the two apparent refractive indices is found for the direction of the applied field; for P(0)–A(90) and the other three equivalent positions, the field of view turns dark. Conoscopic observation now shows a biaxial acute bisectrix-like figure (Figure 1) with which the effective path difference is measured employing a Berek compensator ($0-5\lambda$). To this end, the sample is kept between crossed polarizers P(45)–A(135); the slow axis of the tilting compensator is set along y and the compensator is rotated until the separation between the isogyres reduces to zero or the biaxial figure turns uniaxial. No hydrodynamic motion is seen up to 150 V (the maximum voltage applied).

The graph of measured optical path difference Δl vs square of the applied electric field E^2 for a weak anchoring energy is expected to be a straight line passing through the origin.^{4,6} Our measurements with CNRbis12OBB do not conform to a linear dependence; there exists a downward deviation of the experimental points which is pronounced particularly at elevated voltages (Figure 2). This is explained mainly by the stabilizing action of the negative dielectric anisotropy ($\Delta \epsilon = (\epsilon_{11} - \epsilon_{\perp}) < 0$) of the material which is augmented by the anchoring energy term.⁴ Thus, by taking into account the contributions from the dielectric torque and the anchoring energy term, it is possible to obtain a good linear fit between Δl and the square of the effective field E_{eff}^2 given by eq 3.⁴

Figure 3 presents a plot of flexoelectrically induced Δl as a function of E_{eff}^2 ; E_{eff} is calculated for $d = 22.7 \mu\text{m}$, separation between the electrodes $L = 1.9 \times 10^{-3} \text{ m}$, $\Delta \epsilon = -1.771$, $K_{33} = 2.29 \text{ pN}$ (at 120°C), and various assumed values of W . The best fit was obtained for $W = 1.0 \mu\text{J m}^{-2}$, a typical value expected for silane-coated glass plates.¹⁰ For comparison, in Figure 3 we have also shown the data for $W = 0.5$ and $5.0 \mu\text{J m}^{-2}$ which conform more to a second-order polynomial variation rather than a linear fit through the origin. Further, the ‘coefficient of determination’ $R^2 = 0.9974$ for $W = 1.0 \mu\text{J m}^{-2}$ is the closest

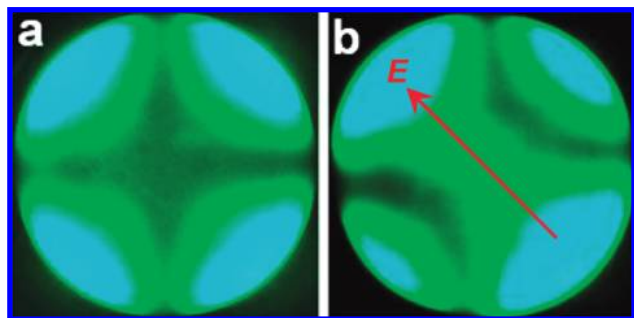


Figure 1. Interference figure under conoscopic observation between crossed polarizers for homeotropic orientation of the director in **CNRbis12OBB** at 120 °C. (a) No electric field applied. (b) In plane field $E = 47.37 \text{ V mm}^{-1}$ applied diagonally as indicated by the arrow.

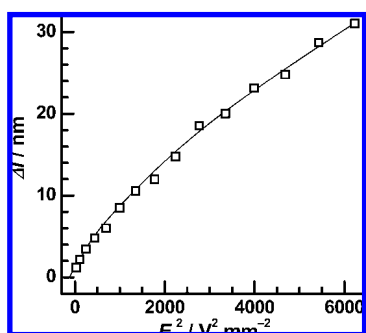


Figure 2. Optical path difference as a function of square of the applied electric field showing a nonlinear variation in **CNRbis12OBB**.

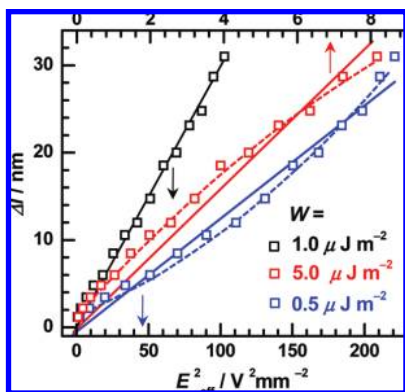


Figure 3. Optical path difference as a function of square of the effective electric field strength for three different assumed values of the anchoring energy W in **CNRbis12OBB**. The continuous lines through the data points are linear fits passing through the origin. The dotted lines correspond to second-order polynomial fits. The bottom x -scale applies to blue and black squares, and the top x -scale applies to red squares.

to unity; thus, we choose the slope $0.29725 \times 10^{-15} \text{ m}^3 \text{ V}^{-2}$ of the corresponding line to obtain the apparent flexocoefficient e_{3x}^* , and with $\Delta n = 0.103$, we find $e_{3x}^* = 3.94 \pm 0.98 \text{ pC m}^{-1}$ at 120 °C. The variation by $\pm 0.98 \text{ pC m}^{-1}$ indicated here corresponds to the difference in Δl for the two directions of the dc field. In view of the symmetric end substituents of **CNRbis12OBB** (dodecyloxy chains), the surface polarization is probably negligible in which case $e_{3x}^* = e_{3x}$.

Finally, we describe the results of our new method for estimating the values of W , e_{3x} and e_+ by measuring the optical path change under simultaneous action of ac and dc fields. Figure 4 illustrates the variation of Δl as a function of E_{eff}^2 , as given by eq 7. Here, $d = 79.7 \text{ } \mu\text{m}$, $L = 1.85 \text{ mm}$, and $T = 120$

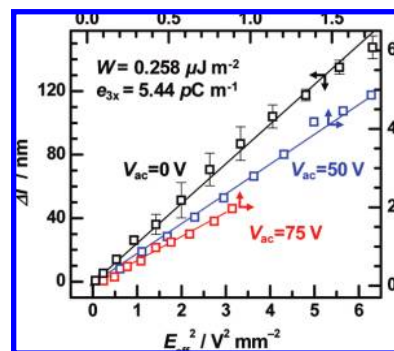


Figure 4. Optical path difference as a function of square of the effective electric field strength in **CNRbis12OBB** for three different cases corresponding to $V_{\text{ac}} = 0, 50, \text{ and } 75 \text{ V}$. The linear fits are for $W = 0.258 \text{ } \mu\text{J m}^{-2}$ corresponding to the highest value of the coefficient of determination R^2 . The lines differ slightly in slope, and the variation in e_{3x} is within $\sim 7\%$.

°C. The best fit of eqs 2 and 7 to the data for all the three cases in Figure 4 is found for $W = 0.258 \text{ } \mu\text{J m}^{-2}$, and the corresponding value of $|e_{3x}|$ is $5.44 \pm 0.37 \text{ pC m}^{-1}$. This value is $\sim 38\%$ greater than the average e_{3x} found with the thinner cell by the classic method. Such a degree of variation is not uncommon in flexomeasurements.¹

The fact that, with a reasonable value of W , it is possible to find a linear fit between Δl and E_{eff}^2 , as in Figures 3 and 4, shows that, for the nematic under discussion, the corrections due to the anisotropic flexo- and elastic coefficients (eq 5) probably cancel each other out, i.e., $\Delta_1 + \Delta_2 \approx 0$, and then, the splay flexocoefficient e_{1z} of the compound can be determined using:

$$e_{1z} = -e_{3x} \left(1 + \frac{8\Delta K}{6K_{33} + 3Wd} \right) \quad (10)$$

Preliminary results indicate ΔK to be $\sim 4 \text{ pN}$ at 120 °C, and the corresponding $|e_{1z}|$ works out to be $\sim 7.74 \text{ pC m}^{-1}$.

B. The Flexocoefficients in BCCB. As previously remarked, in **BCCB** in view of its positive dielectric anisotropy, it is possible to evaluate W by studying the quenching of surface polar instability, employing the longitudinal sample geometry. We observed the surface polar instability in **BCCB** to occur always at the cathode (Figure 5); with reversal of the field, there was a corresponding shift in the focal plane of the instability. The linear increase of the dc instability threshold, as a function of the simultaneously applied dielectrically quenching ac field (Figure 6), provides both e_+^* and b . Linear fit to the data points in Figure 6 yields $V_{\text{dc}}^0 = 2.022 \pm 0.16 \text{ V}$, and from the slope $0.672 (\pm 0.042)$ of the line, we calculate $\Delta V_{\text{dc}} = 3.36 \pm 0.21 \text{ V}$, for $V_{\text{ac}} = 5 \text{ V}$. Thus we obtain, using eqs 8 and 9, $b = 1.4 \pm 0.2 \text{ } \mu\text{m}$ and $e_+^* = -34.0 \pm 2.1 \text{ pC m}^{-1}$. The negative sign here arises from the location of the instability at the cathode.¹³

Now we may consider the determination of the apparent flexocoefficient e_{3x}^* . Figure 7 presents a plot of flexoelectrically induced Δl as a function of E_{eff}^2 ; E_{eff} is calculated for $d = 6 \text{ } \mu\text{m}$, $L = 0.95 \times 10^{-3} \text{ m}$, $\Delta n = 0.16658$, $\Delta \epsilon = 5.744$ (at 1 kHz), $K_{33} = 3.956 \text{ pN}$, and $K_{11} = 12.54 \text{ pN}$ (all material parameters measured¹⁴ at 140 °C). Fitting data points to eq 5 and using $b = 1.4 \text{ } \mu\text{m}$ from the quenching data, we get $|e_{3x}^*| = (51.56 \pm 0.63) \text{ pC m}^{-1}$ and $e_+ = \pm (34.83 \pm 0.39) \text{ pC m}^{-1}$, the positive sign applying when e_{3x}^* is negative and vice versa.

Thus, for positive e_{3x}^* or, equivalently, negative e_+ , we get the set of values

$$m_p = +0.83 \text{ pC m}^{-1}, e_{3x} = +50.8 \text{ pC m}^{-1},$$

$$\text{and } e_{1z} = -85.6 \text{ pC m}^{-1} (\text{first set}),$$

and for negative e_{3x}^* or, equivalently, positive e_+ ,

$$m_p = -68.8 \text{ pC m}^{-1}, e_{3x} = +17.2 \text{ pC m}^{-1},$$

$$\text{and } e_{1z} = +17.6 \text{ pC m}^{-1} (\text{second set})$$

Now we may consider the two possible situations $m_p > 0$ and $m_p < 0$. The first choice implies that the alkyl residue of the bent core fragment interacts with the substrate, while the calamitic fragment containing the cyano group is oriented away from the surface; this corresponds to the hypothesis of ref 11 that biphilic nematic molecules interact with a silanized (hydrophobic) surface with their hydrophobic ends. On the contrary, negative m_p corresponds to the cyano group in contact with the glass, i.e., the biphilic molecules enter the molecular vacancies (holes) in the silane coating and are oriented with respect to the glass just the same way as the biphilic silane (alternative hypothesis employed in ref 15). It is well-known that molecular holes are obligatory for a good homeotropic orientation. A densely packed surfactant layer does not orient a nematic at all. We may now consider an argument favoring the negative sign for m_p . The surface polarization for cyanobiphenyls was evaluated as $\sim 170 \text{ pC m}^{-1}$ (ref 7) showing that all the cyano dipoles are ferroelectrically ordered along the layer normal at the substrates. For the first set of solutions, m_p is practically zero and does not match this evaluation at all. For the second set, m_p is in a good accord with the quoted value, in view also of the larger cross section of **BCCB** molecules. Additional arguments in favor of the second set of solutions comes from the cluster model.

Cluster Model of Bent-Core Nematic Flexoelectricity

According to the statistical theory^{16,17} of single-molecule dipolar flexoelectricity, e_{3x} is expected^{2,3,5} to be always less than a few tens of pC m^{-1} . On the other hand, the marked steric and electric asymmetry of bent-core nematics is most probably fully compensated in a uniaxially ordered nematic phase.¹⁸ This would result in some kind of molecular clustering. According to the existing data,¹⁹ bent-core nematics are highly clustered systems. Figure 8 depicts a cluster consisting of a chain of n (an even number) compensated bent-core molecules, each with a transverse dipole moment μ and length l . Such a chain of antiparallel dipoles is a strong candidate for quadrupolar flexoelectricity.^{1,20,21} In the reference frame in Figure 8, the quadrupolar moment tensor of the cluster has only two nonzero components:

$$Q_{xz} = Q_{zx} = (3/2)[\mu l/2 + \mu 3l/2 + \dots + \mu(n-1)l/2] =$$

$$3\mu l n^2/16 \quad (11)$$

It is remarkable that the quadrupolar moment scales as the square of the number of molecules in the cluster. If we diagonalize the tensor, the following diagonal components are obtained:

$$Q_{x'x'} = Q_{xz}, \quad Q_{y'y'} = 0, \quad Q_{z'z'} = -Q_{xz} \quad (12)$$

i.e., the anisotropy of the quadrupole moment is given by:

$$\Delta Q = Q_{z'z'} - (Q_{x'x'} + Q_{y'y'})/2 = -3Q_{xz}/2 = -9\mu l n^2/32 \quad (13)$$

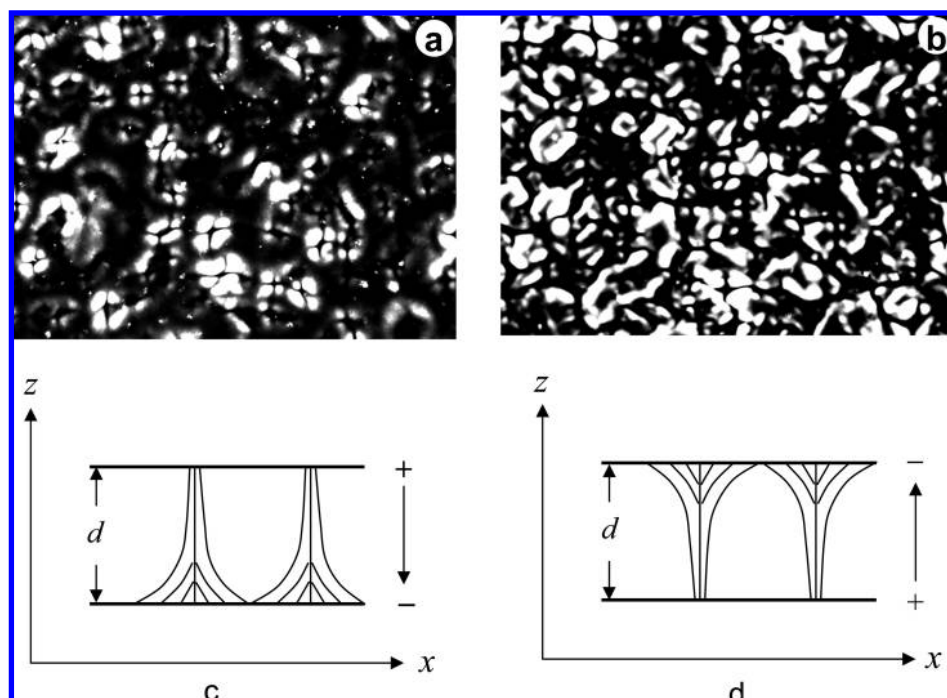


Figure 5. Microphotographs of surface instability under crossed polarizers in **BCCB** at 4.3 V dc; $d = 14.7 \mu\text{m}$, and $T = 140^\circ\text{C}$. Distortion pattern always forms at the negative electrode (cathode instability). (a) $E = -0.3 \text{ V } \mu\text{m}^{-1}$; bottom electrode negative. (b) $E = +0.3 \text{ V } \mu\text{m}^{-1}$; top electrode negative. The focal plane separation between (a) and (b) is $15.47 \mu\text{m}$ (i.e., to capture (b), the microscope stage was shifted down with respect to (a) by this distance), which closely matches with the cell thickness.

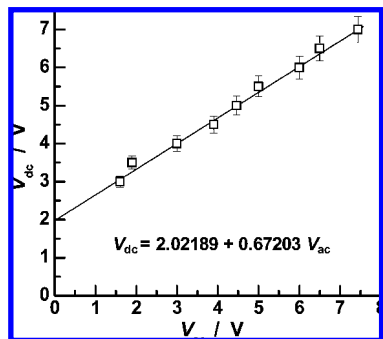


Figure 6. Dielectric quenching of the surface instability: The dc instability threshold as a function of the ac stabilizing field. The line is a linear fit to the data yielding V_{dc}^0 and ΔV_{dc} at any given V_{ac} .

Then, according to refs 20 and 21, the quadrupolar flexo-coefficients are given by:

$$e_{1z} = -L_{zz}N_0S\Delta Q/3, \quad e_{3x} = -L_{xx}N_0S\Delta Q/3 \quad (14)$$

where N_0 is the volume density of quadrupoles, S is the degree of ordering, and L_{xx} and L_{zz} are the corresponding components of the Lorentz field tensor. The number of quadrupoles equals the number of clusters, that is $N_0 = N/n$, where N_0 is the volume density of bent-core molecules and n is the number of molecules in the cluster. Thus, we finally arrive at

$$e_{1z} = 3L_{zz}NS\mu\ln/32, \quad e_{3x} = 3L_{xx}NS\mu\ln/32 \quad (15)$$

We see that the values of both flexocoefficients scale linearly as n , the number of clustered molecules. L_{xx} and L_{zz} are both close to 1, so that, with typical values of $\mu = 1 \times 10^{-29}$ C m, $l = 10$ nm, $S = 0.5$, and $N = 10^{27}$ m $^{-3}$, we get $e = 10$ pC m $^{-1}$ for $n = 2$. This value nearly matches the result obtained for **CNRbis12OBB** and perhaps also the second set of coefficients for **BCCB**, if we take into account that in a cluster of two **BCCB** molecules, there will be two additional, antiparallel, and widely spaced dipole moments of the end cyano groups. The approximately equal values of the two **BCCB** flexocoefficients (cf. second set) are further evidence in favor of their quadrupole origin.^{20,21} It is to be noted, however, that the conditions for formation of a chain-like 1D cluster of $n > 2$ with sickle-type molecules are not optimal. Some other type of nonpolar clustering might contribute to a giant flexo in **BCCB**, if any. Incidentally, an important feature of **CNRbis12OBB** is its negative conductivity anisotropy throughout the nematic range; this pretransitional effect is as in hepyloxy azoxybenzene (**HOAB**)²² and points to a SmC-like short-range order. This should be kept in mind while discussing the cluster model for **CNRbis12OBB**. For example, the opposite signs of the two **CNRbis12OBB** flexocoefficients inferred from eq 9 are not in accordance with a quadrupolar mechanism, which requires the coefficients to be positive. A dipole contribution that can be of either sign could also be involved.

Furthermore, one needs a value of $n > 200$ (a feasible number) to attain flexocoefficients in the nC m $^{-1}$ range for a 1D chain-type of nonpolar clustering. Similar, although mathematically more involved, conclusions for the quadrupole flexoelectricity of 2D clusters of a planar, smectic-like character could be drawn,

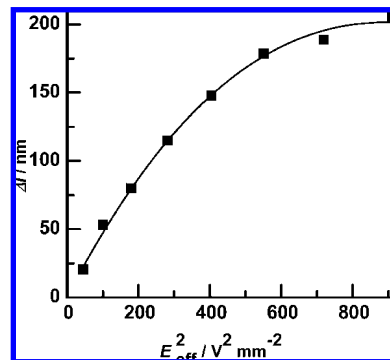


Figure 7. Optical path difference versus square of the effective electric field strength for **BCCB** ($b = 1.4$ μm from Figure 6).

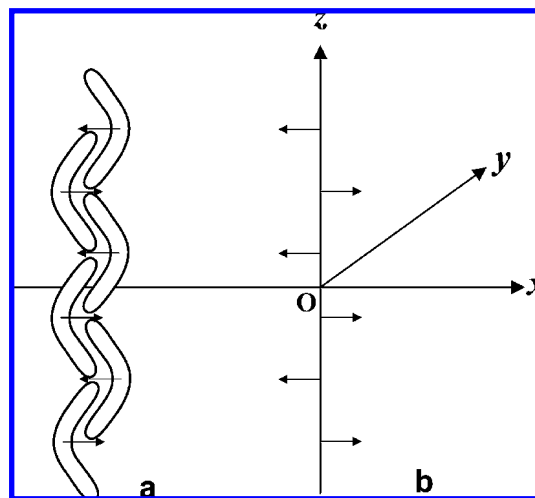


Figure 8. A linear nonpolar cluster model of bent-core molecules. The dipolar-type steric and electric asymmetry of individual molecules is fully compensated in the cluster. Therefore, the cluster possesses an electric asymmetry of quadrupole-type only: the longer the cluster, the larger the quadrupole moment. The quadrupole scales like the second power of n , the number of molecules in the cluster; thus, the quadrupole density of the liquid crystal and its flexoelectric coefficients scale linearly with n .

pointing out that the origin of giant flexoelectricity of bent cores should be traced down to the quadrupolar clustering. A simple case of antiferroelectric ordering of transverse dipoles in adjacent smectic layers in a cluster directly follows from the 1D model above by replacing μ with the total layer polarization $m\mu$, where m is the number of banana molecules in the layer, and $l/2$ by l , where l is now the layer thickness. The quadrupolar moment of such an antiferroelectric smectic cluster could be substantial. Large clusters are evidenced by unusual, very slow fluctuations in polarized scattering, which suggests that the bent-core nematic has a “glassy” character. Dilution of a bent core in a calamitic solvent indicates a dramatic development of the glassy dynamics between 30 and 60 wt % of the bent-core component. The slow dynamics is the result of a combination of ordinary fluid nematic with a frustrated network of more closely packed (perhaps smectic-like) domains.¹⁹ The observation of giant flexoresponse well above the clearing point^{2,3} is another indication of quadrupolar flexoelectricity (the clusters may display a sufficient size even above the nematic–isotropic temperature, gradually disappearing with the temperature rise). The model analyzed above assumes the whole nematic as clustered in just one type of clusters. This may not be the case in the entire nematic range, as evidenced by the temperature dependence.^{2,3} A mixture of clusters and monomers would then be a nonhomogeneous

system where the validity of Maxwell relations (requiring equality of both direct and converse flexocoefficients) may call for a special consideration. One might imagine a case where nonpolar clusters react chiefly to mechanical deformations which polarize them, while polar monomers react chiefly to electric fields. However, note in this respect that, not only the direct flexoeffect reported in ref 2 but also the converse flexoeffect reported in ref 3 are both giant and in good accord, even with respect to the temperature dependence.

It is, therefore, a nontrivial question as to why the giant flexoelectric effect is only observable in some experimental situations but not in others. This giant discrepancy is far from being resolved and needs further investigations. This study provides only some clues toward its understanding. We recognize an important difference between two types of measurements, one involving flexible electrodes and the other involving rigid electrodes. In macroscopic terms, the mechanically free and clamped layers are thermodynamically nonequivalent.¹⁷ In molecular terms, we may explore the size of the cluster that responds to a particular type of external field, steric or electric. When a bent-core nematic sample is confined between flexible electrodes, the conditions for a response of large quadrupole clusters as a whole may be optimal. This is to be contrasted against the case of a rigid electrode confinement wherein the clusters may be disintegrated because of the incompatibility of much larger flexodeformation with the rigid confinement. It seems clear enough that in a clamped sample large deformations are suppressed. Thus, the idea is that clusters may become disintegrated in the clamped case in response to internal strains that cannot otherwise be relaxed.

Another reason might be a much longer relaxation time for disintegration of large clusters into quadrupole dimers, which is more relevant to a dc excitation, as in ref 5 as well as the present study. A special, very low relaxation frequency of forced flexoelectric oscillations^{21,23,24} could then be expected.

Conclusions

Flexoelectric-bending deformation of a homeotropic layer due to an inplane electric field is analyzed for two bent-core nematics with opposite signs of $\Delta\epsilon$. Through simultaneous application of dc and ac fields, dielectric suppression of flexoelectric-bending in the mesogen with $\Delta\epsilon < 0$ and quenching of surface polar instability in that with $\Delta\epsilon > 0$ are achieved; thus the anchoring energies required for estimation of the flexocoefficients are obtained. On the theoretical side, to analyze the results of deformations produced under considerable dielectric and anchoring effects, the Helfrich theory is extended taking higher order distortions into effect. This has enabled extraction of the splay coefficient e_{1z} as well. Both the flexoelectric constants are found to be of the usual order of magnitude; this result assumes significance in view of a recent finding of giant flexoelectric bending in a different BC mesogen. A model of

nonpolar clusters with quadrupolar flexoelectricity is advanced in an attempt to explain these widely differing values obtained under different conditions. Further experiments are planned to test the general validity of the cluster hypothesis as well as the analytical approach developed here.

Acknowledgment. This study is carried out under the Indo-Bulgarian joint research project (No. INT/BUL/B-75/07) supported by the Department of Science and Technology, New Delhi, and the Ministry of Education and Science, Scientific Studies Fund of Bulgaria. We thank Professor K.A. Suresh for the experimental facilities and support.

References and Notes

- (1) Petrov, A. G. Measurements and interpretation of flexoelectricity. In *Physical Properties of Liquid Crystals: Nematics*; Dunmur, D. A., Fukuda, A., Luckhurst, G. R., Eds.; INSPEC-IEEE: London, 2001; Chapter 5, pp 251–264.
- (2) Harden, J.; Mbang, B.; Eber, N.; Fodor-Csorba, K.; Sprunt, S.; Gleeson, J. T.; Jakli, A. *Phys. Rev. Lett.* **2006**, *97*, 157802.
- (3) Harden, J.; Teeling, R.; Gleeson, J. T.; Sprunt, S.; Jakli, A. *Phys. Rev. E: Stat., Nonlinear, Soft Matter Phys.* **2008**, *78*, 031702.
- (4) Helfrich, W. *Phys. Lett. A* **1971**, *35*, 393.
- (5) Le, K. V.; Araoka, F.; Fodor-Csorba, K.; Ishikawa, K.; Takezoe, H. *Liq. Cryst.* **2009** (in press).
- (6) Schmidt, D.; Schadt, M.; Helfrich, W. *Z. Naturforsch. A* **1972**, *27*, 277.
- (7) Lavrentovich, O. D.; Nazarenko, V. G.; Sergan, V. V.; Durand, G. *Phys. Rev. A: At., Mol., Opt. Phys.* **1992**, *45*, R6969.
- (8) Kovalenko, L.; Schroder, M. W.; Reddy, R. A.; Diele, S.; Pelzl, G.; Weissflog, W. *Liq. Cryst.* **2005**, *32*, 857.
- (9) Yelamagad, C. V.; Krishna Prasad, S.; Nair, G. G.; Shashikala, I. S.; Shankar Rao, D. S.; Lobo, C. V.; Chandrasekhar, S. *Angew. Chem., Int. Ed.* **2004**, *43*, 3429.
- (10) Blinov, L. M.; Kabayenkov, A. Yu.; Sonin, A. A. *Liq. Cryst.* **1989**, *5*, 645.
- (11) Haas, W.; Adams, J.; Flannery, J. B. *Phys. Rev. Lett.* **1970**, *25*, 1326.
- (12) Petrov, A. G.; Derzhanski, A. *Mol. Cryst. Liq. Cryst. Lett. Sect.* **1977**, *41*, 41.
- (13) Petrov, A. G.; Mitov, M.; Derzhanski, A. *J. Phys. (Paris)* **1978**, *39*, 273.
- (14) Kumar, P.; Hiremath, U. S.; Yelamagad, C. V.; Rossberg, A. G.; Krishnamurthy, K. S. *J. Phys. Chem. B* **2008**, *112*, 9753.
- (15) Kühnau, U.; Petrov, A. G.; Klose, G.; Schmiedel, H. *Phys. Rev. E: Stat., Nonlinear, Soft Matter Phys.* **1999**, *59*, 578.
- (16) Helfrich, W. *Z. Naturforsch. A* **1971**, *26*, 833.
- (17) Derzhanski, A.; Petrov, A. G. *Phys. Lett. A* **1971**, *36*, 483.
- (18) Derzhanski, A.; Petrov, A. G. *Mol. Cryst. Liq. Cryst.* **1982**, *89*, 339.
- (19) Dorjgotov, E.; Fodor-Chorba, K.; Gleeson, J. T.; Sprunt, S.; Jakli, A. *Liq. Cryst.* **2008**, *35*, 149.
- (20) Stojadinovic, S.; Adorjan, A.; Sprunt, S.; Sawade, H.; Jakli, A. *Phys. Rev. E: Stat., Nonlinear, Soft Matter Phys.* **2002**, *66*, 060701.
- (21) Prost, J.; Marcerou, J. P. *J. Phys. (Paris)* **1977**, *38*, 315.
- (22) Derzhanski, A.; Petrov, A. G. *Acta Phys. Pol. A* **1979**, *55*, 747.
- (23) Rondelez, F. *Solid State Commun.* **1972**, *11*, 1675.
- (24) Petrov, A. G.; Ionescu, A. Th.; Versache, C.; Scaramuzza, N. *Liq. Cryst.* **1995**, *19*, 169.
- (25) Marinov, Y.; Shonova, N.; Naydenova, S.; Petrov, A. G. *Mol. Cryst. Liq. Cryst.* **2000**, *351*, 411.

JP903241Z